AIR FORCE FLIGHT DYNAMICS LABORATORY
DIRECTOR OF LABORATORIES
AIR FORCE SYSTEMS COMMAND
WRIGHT PATTERSON AIR FORCE BASE OHIO

MODEL INJECTION SYSTEM INDUCED ACCELERATIONS IN THE

RENT TEST LEG OF THE 50 MEGAWATT FACILITY

By

Dr. Lawrence A. Walchli

September 1973

Flight Mechanics Division
Air Force Flight Dynamics Laboratory·
Wright-Patterson AFB, Ohio 45433

20000503 093

SUMMARY

The Re-Entry Nose Tip (RENT) test leg of the 50 Megawatt Electrogas-dynamics Facility has the capability of testing models which have been rapidly inserted into the test stream. Normal ranges for the insertion speeds are up to 40 inches per second in a transverse direction and up to 25 inches per second in an axial direction. Acceleration data has been recorded and analyzed in this document in order to provide a broad spectrum of data which can be used as a guide for the structural design of future test articles and their sometimes delicate instrumentation.

The supportive efforts of AFFDL/FXN are appreciated and, in particular, those of Messers Charles W. Wood, Alan G. Blore and Carl F. Welhener. Special thanks are extended to Robert E. Stewart for preparing the figures for this report.

This Technical Memorandum has been reviewed and is approved.

PHILIP P. ANTONATOS
Chief, Flight Mechanics Division
Air Force Flight Dynamics Laboratory

TABLE OF CONTENTS

Page

ILLUSTRATIONS

iii

I. INTRODUCTION

The Re-Entry Nose Tip (RENT) test leg of the 50 Megawatt Facility is used for hyperthermal testing of nose tips under simultaneous conditions as high as 100 atmospheres impact pressure and 18,000 BTU/ft^2 sec heat flux to a 0.25 inch radius nose tip. Such extreme conditions normally require very rapid carriage movement to avoid either total destruction of a model which has been designed to sweep through the test gas flow or significant shape change of an ablation model before it has been pinned at the desired testing position. Accompanying these rapid carriage movements are large accelerations and decelerations which must be considered in the structural design of test articles. Past practice has been to structurally overdesign the models so that they would survive even the most severe g-loadings which the model injection system might impose on them.

During October, 1972 a new type of testing was initiated in the RENT test leg-thermostructural testing. The nature of thermostructural testing requires the models and particularly their instrumentation to be rather fragile.

The work documented in this report was performed to support this new type of testing. A complete matrix of acceleration/deceleration data over the anticipated operating range of the model support system is reported. This data can then be used for model and instrumentation design for future thermostructural tests in the RENT test leg of the 50 Megawatt Facility.

II. EXPERIMENTAL PROCEDURE

The model injection system of the RENT test leg has the capability of moving five consecutive models transversely into or through the test flow at speed as high as 100 inches per second. Normal operating speeds are generally below 40 inches per second. When models are pinned on nozzle centerline, the system has the capability of axially driving the model in one of two modes. For ablation models whose nose tips must be held within the test rhombus of the flow field, two light sensors are used to control a hydraulic servo system which in turn axially drives the model forward at a rate equal to the recession rate of the ablative nose tip. For non-ablating models, the axial drive system performs in a two-position mode whereby the model is driven to a prescribed position and held. Normal speed range of the latter mode is up to 25 inches per second. Since the purpose of this test program is to acquire and analyze acceleration data for support of non-ablative thermostructural testing, only the transverse carriage motion and the two-position mode axial drive have been considered.

The data presented herein were generated by operating the carriage through a normal operating sequence. The arc heater was not being operated although several sets of data recorded during "hot" runs showed that all acceleration data was totally independent of arc heater operation.

The instrument used to monitor the carriage accelerations was a Statham Model A8-10-335 strain gauge bridge type accelerometer whose output was linear in the range ± 10 g's. The output signal was obtained

by a CEC 20 kilohertz (khz) carrier system and recorded on a Visicorder oscillograph. The bandwidth of the system was 2 khz.

Five different accelerations were monitored during transverse strut movement, viz. initial carriage start, hydraulic stop on nozzle centerline using the hydraulic valves to isolate the oil in the drive cylinder, pin stop on centerline, re-acceleration of the carriage leaving the pinned position and the shock absorber stop at conclusion of the carriage sweep. Several of these outputs were successfully dissected during the course of the investigation resulting in a more thorough understanding of the complicated noise and mechanical accelerations experienced by the models.

Three different accelerations were monitored during axial strut movement, viz. initial start and final hydraulic and mechanical stops. Analyses of the experimental results are presented in the next section.

In all cases the accelerometer was mounted on the base of strut 5 which in turn was mounted on the moving carriage. The output signal was accepted as an absolute value with respect to a set of earth-fixed coordinates. Possible movement of the carriage mounting base was not considered.

III. DISCUSSION OF RESULTS

III.A. General Description of the Acceleration/Deceleration Pattern Through A Carriage Traverse

Carriage movement is initiated by opening one or more control valves in the hydraulic system. Acceleration to the prescribed carriage speed follows. Maximum acceleration occurs approximately 50 milliseconds (msec) after the beginning of carriage movement.

The beginning of deceleration at the specified strut is initiated by closing the isolation valves on the two ends of the hydraulic drive cylinder. Maximum deceleration occurs about 35 msec later as the carriage comes to a temporary halt. As rebound begins, the acceleration again begins to build. This process is suddenly interrupted by the impact of the tapered pin against the edge of the strut alignment hole in the undercarriage. The result is a jerk i.e., the first derivative of the acceleration. The maximum acceleration in the pinning maneuver occurs about 5 msec after the jerk starts. The subsequent acceleration/ deceleration pattern is too complex to successfully dissect but in general the completion of the pinning process requires another 80 to 100 msec depending on the amount of hole/pin misalignment at the beginning of the pinning process.

Several hundred msec after pinning has occurred, the hydraulic locking valves on the head and rod ends of the main cylinder are released. When the prescribed dwell time on a model has been satisfied, a simultaneous signal is sent by the Agastat programmer to de-pressurize the rod end of the cylinder and to pull the alignment pin. The pin retraction governs

4

the termination of dwell and the carriage again accelerates to a prescribed velocity.

The above sequence of events is repeated until unpinning of the final strut has occurred and the carriage again is put into motion.

The final deceleration occurs when the carriage encounters a shock absorber and comes to rest. This deceleration occurs over a four inch length of shock absorber compression.

III.A.1. Initial Acceleration

Figure 1 is a reproduction of a selected acceleration and carriage position trace which clearly shows specific details of the initial acceleration. The accelerometer was mounted on the base plate of strut 5, with its axis of maximum sensitivity parallel to the transverse motion of the carriage. The position trace is output from a single-turn potentionmeter whose accuracy is within ± 1%.

About 50 msec prior to carriage movement the hydraulic valving was activated, thereby producing noise on the accelerometer output trace. This noise had two measurable frequencies. The fundamental frequency was about 72 hertz (hz) and the first overtone was 144 hz. The maximum amplitude of the noise signal was equivalent to about 0.8 g of acceleration and was associated with the fundamental frequency.

By the time the carriage began to move, this noise signal attenuated sufficiently so as to make the actual mechanical acceleration of the carriage clearly discernible. About 50 msec after the carriage began to move, it experienced maximum g-loading. The maximum acceleration recorded on this particular trace was about 0.85 g.
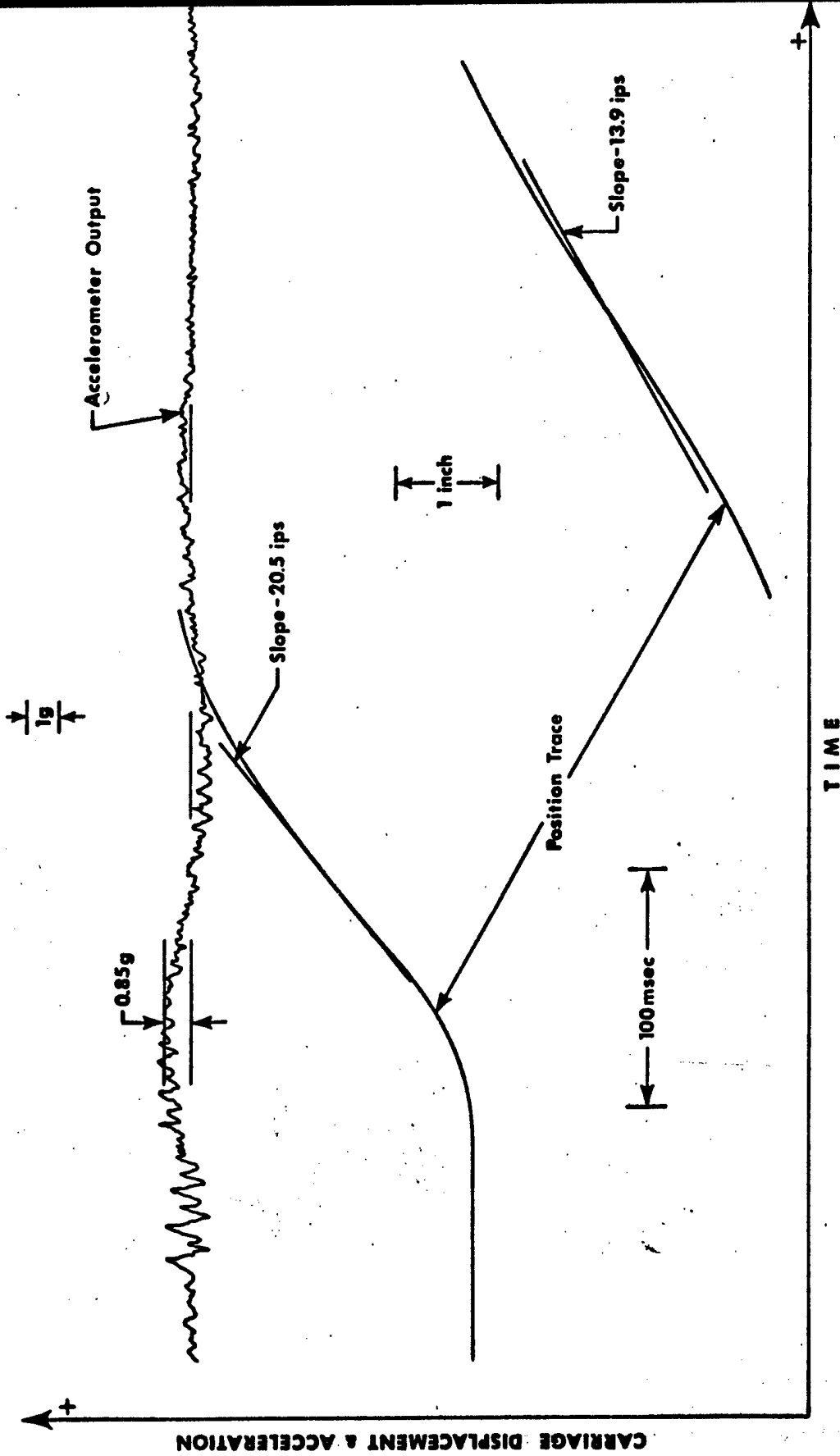
5

FIGURE 1. INITIAL TRANSVERSE ACCELERATION

Table 1 summarizes the maximum g-loadings produced by accelerating the carriage from rest to several different final velocities. The accelerations were seen to be a direct function of the maximum speed attained by the carriage. The data confirmed that all periods of maximum acceleration occurred about 50 msec after first carriage movement. Hence, to attain an increased velocity during a constant elapsed time the carriage had to experience increased accelerations.

One further point of interest regarding the position and acceleration traces in Figure 1 is the cyclic nature of the actual carriage acceleration. For all normal carriage speeds, i.e., up to 40 inches per second (ips), the carriage accelerated to maximum velocity during the first 115 msec at which time the acceleration dropped to zero. The maximum velocity attained was higher than the final steady state value. The ratio of maximum to steady state is defined as velocity overshoot. During the next 115 msec the carriage slowed, producing a deceleration. A small acceleration over a third period of 115 msec produced the final steady state carriage speed. The frequency of this cyclic acceleration appeared to be independent of final carriage speed for all speeds below 40 ips. The cyclic motion may have been caused by alternate compression and rarefaction of some residual air trapped within the hydraulic system or possibly by cyclic movement of the spools in the flow control valves. The magnitude of the velocity overshoot is shown in the middle column in Table 1.

At carriage speeds near 40 ips the carriage velocity overshoot decreases to zero. As the speed is further increased the carriage position trace becomes a monotonically increasing function until the final

TABLE 1.   CARRIAGE INITIAL ACCELERATION

Carriage Velocity (i p s)	Velocity Overshoot	Acceleration (g)
3.12	1.51	0.20
8.87	1.55	0.65
13.9 (Fig 1)	1.48	0.85
17.4	1.45	1.05
19.4	1.38	1.05
19.5	1.57	1.10
19.8	1.44	1.15
22.9	1.35	1.20
25.5	1.33	1.30
26.7	1.22	1.35
28.4	1.24	1.35
35.2	1.17	1.50
37.0	1.12	1.75
39.4	1.06	1.65
49.4	-	1.88
65.4	-	2.00

CARRIAGE INITIAL ACCELERATION

maximum carriage speed is attained. This stabilization time is about equal to the time for the cyclic motion to decay at the lower speeds.

III.A.2. Interim Deceleration

Interim decelerations occur at each model strut designated for pinning. The deceleration process is initiated by hydraulically isolating the main drive cylinder and is terminated by seating a steel pin in an alignment hole located on the lower part of the model support carriage. Since the accelerometer output signal was influenced by several factors in this deceleration, an attempt is made below to identify the various acceleration components.

III.A.2.a. Hydraulic Isolation

Figure 2 depicts the decelerations caused solely by suddenly closing the main cylinder isolation valves. Again, the accelerometer was mounted with its sensitive axis parallel to carriage movement. For a carriage speed of around 14 ips, maximum deceleration was about 1.65 g. Superimposed on the accelerometer output was a small amplitude noise signal whose frequency was about 144 hz. As Figure 2 shows, the initial deceleration was followed by a mild acceleration of about 1.50 g and a second deceleration of about 1.0 g. The carriage position trace showed similar deflections of exactly the same frequency, viz. 14 hz. This movement can probably be attributed to oscillation of the piston in the drive cylinder caused by consecutive compression and rarefaction of the air trapped inside the cylinder. Decelerations were recorded over a range of carriage speed and are presented in Table 2. The results show that while g-loading was strongly dependent on carriage velocity, the mechanical oscillation frequency was constant.
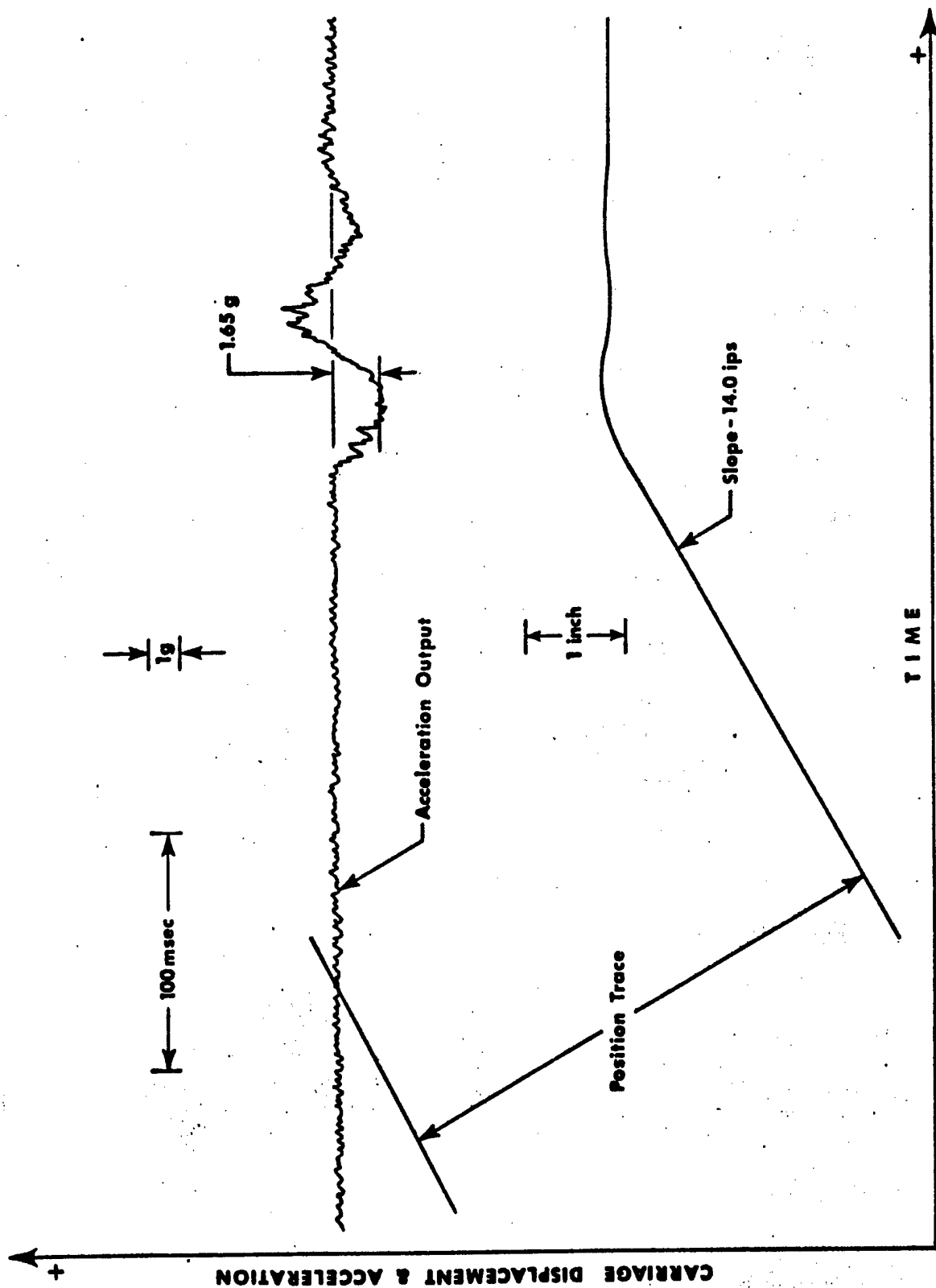
9

FIGURE 2. INTERIM HYDRAULIC DECELERATION

10

TABLE 2 HYDRAULIC ISOLATION INDUCED G-LOADS

Carriage Velocity (1 p s)	Oscillation Frequency (Hz)	Peak Deceleration (g)
2.94	–	0.60
9.10	13.5	1.20
14.0	14.0	1.65
20.4	13.9	2.60
28.8	14.7	3.75
38.4	14.3	5.65

11

III.A.2.b. Pin Insertion

Insertion of the strut alignment pin produces a complex pattern of accelerations and decelerations. The pinning process is strongly dependent on the amount of pin/hole misalignment at the beginning of insertion. The farther the hole is uncentered, the higher are the g-loadings produced by the pin in striking the hole and dragging the carriage into alignment.

As the tapered pin strikes the edge of the hole, accelerations are produced by the lateral movement of the carriage and by the impact of the pin itself. The resultant signal as measured by the accelerometer is a complex superposition of the two effects. In order to better understand the nature of this acceleration the component associated with pin impact has been more closely examined.

Figure 3 shows a typical pin impact acceleration created by driving the pin into the bottom of the carriage substructure. Since the pin was not striking the edge of the alignment hole no transverse carriage motion resulted. The measured impact acceleration should, of course, exceed that produced under real test conditions when the pin actually strikes the edge of the hole in a glancing blow.

The accelerometer was mounted in a vertical position, with its axis of maximum sensitivity parallel to the axis of pin movement. The resultant impact created a g-load of almost 12 g. The various frequencies appearing on Figure 3 were fairly random.

The next step was to precisely align the hole directly over the pin and lock the carriage in position so that the pin could not strike the edge of the hole. Pin actuation would then produce g-loads
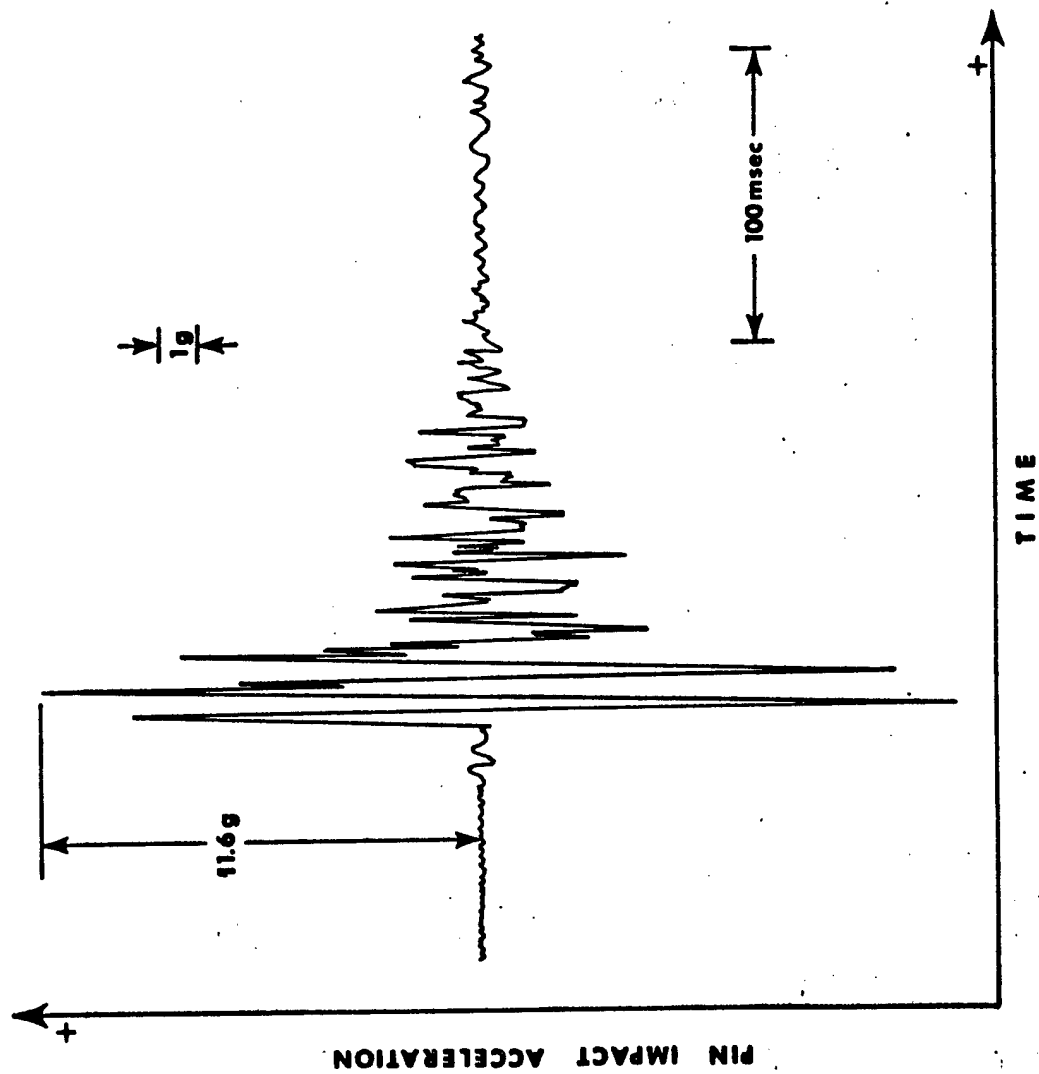
FIGURE 3. PIN IMPACT ACCELERATION, PIN STRIKING BAR VERTICALLY

which would be significantly less than under actual test conditions.

Figure 4 is a facsimile of the acceleration signal produced by the accelerometer when the pin and hole were aligned. The first portion of the output trace represents the accelerations caused by the pin sliding against the wall of the hole. This sliding occurred for about 70 msec before the pin began and then decreased to zero as the pin came to rest. The frequencies appearing on the accelerometer signal were again random.

The data presented in Figures 3 and 4 represents the upper and lower limits of vertical acceleration caused by pin impact. The actual impact acceleration produced by the pin striking a glancing blow on the edge of the alignment hole would generally fall between the 12 g maximum and the 1.3 g minimum.

Figures 3 and 4 represent accelerometer outputs when the instrument was mounted in a vertical position. Since this was the orientation which produced maximum response to the accelerations caused by the vertical pinning process, it facilitated data analysis. However, the primary concern in this phase of the investigation was to dissect the resultant transverse acceleration signal.

The accelerometer was rotated into a plane where its axis of maximum sensitivity was parallel to that along which the carriage ordinarily moved. The static pin impact tests were repeated. The results showed that when mounted transversely the accelerometer sensed accelerations ranging from 0.5 to 4.3 g resulting solely from pin impact.
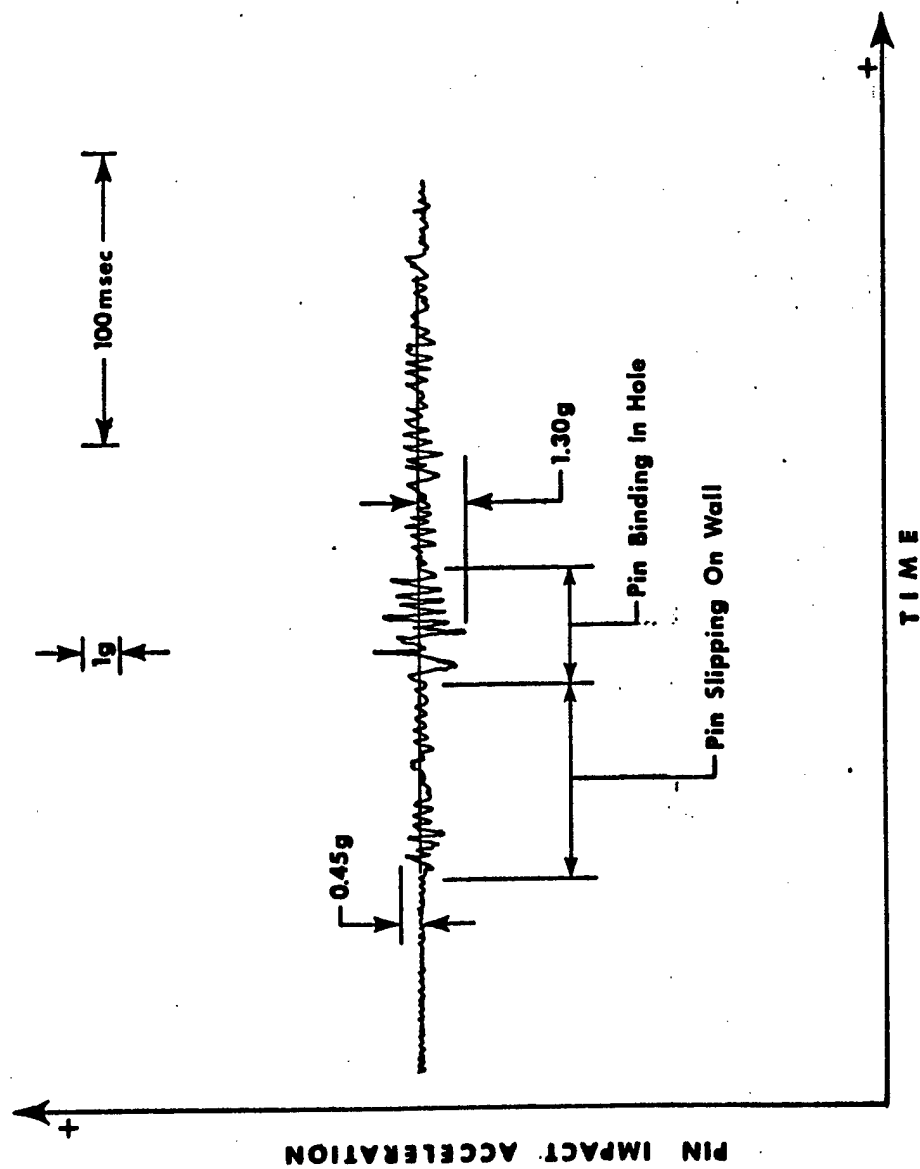
14

FIGURE 4. PIN IMPACT ACCELERATION, PIN ENTERING ALIGNMENT HOLE

The pin insertion study shows that although the highest impact accelerations occur in a vertical direction, transverse accelerations ranging from 0.5 to 4.3 g (a factor of almost 9 to 1 between maximum and minimum g-loading) result because of mechanical coupling within the carriage substructure.

III.A.2.c. Resultant Interim Deceleration

The superposition of the aforementioned accelerations and decelerations which occur when each strut is pinned on the nozzle centerline results in a highly complex accelerometer signal. A selected example is shown in Figure 5. This trace was produced by a transversely oriented accelerometer when the carriage was decelerated from a transverse velocity of 14.0 ips and pinned.

A composite structure of such an output signal is shown in Figure 6. The scales of both the ordinate (acceleration) and abscissa (time) have been expanded. Included are typical isolated traces for hydraulic deceleration of the moving carriage, impact accelerations for the pin against the stationary carriage and into the stationary aligned hole and the combined acceleration signal. All signals represent output from a transversely oriented transducer. The component which is missing from the composite is the transverse acceleration resulting when the force of the pin drags the carriage into centerline alignment.

The time and amplitude of the impact acceleration signals change significantly from one run to another or even from one strut to another on a given run depending on pin/hole misalignment at impact. The pin impact acceleration indirectly depends on carriage speed only because the higher the speed the more probable is a large pin/hole misalignment.
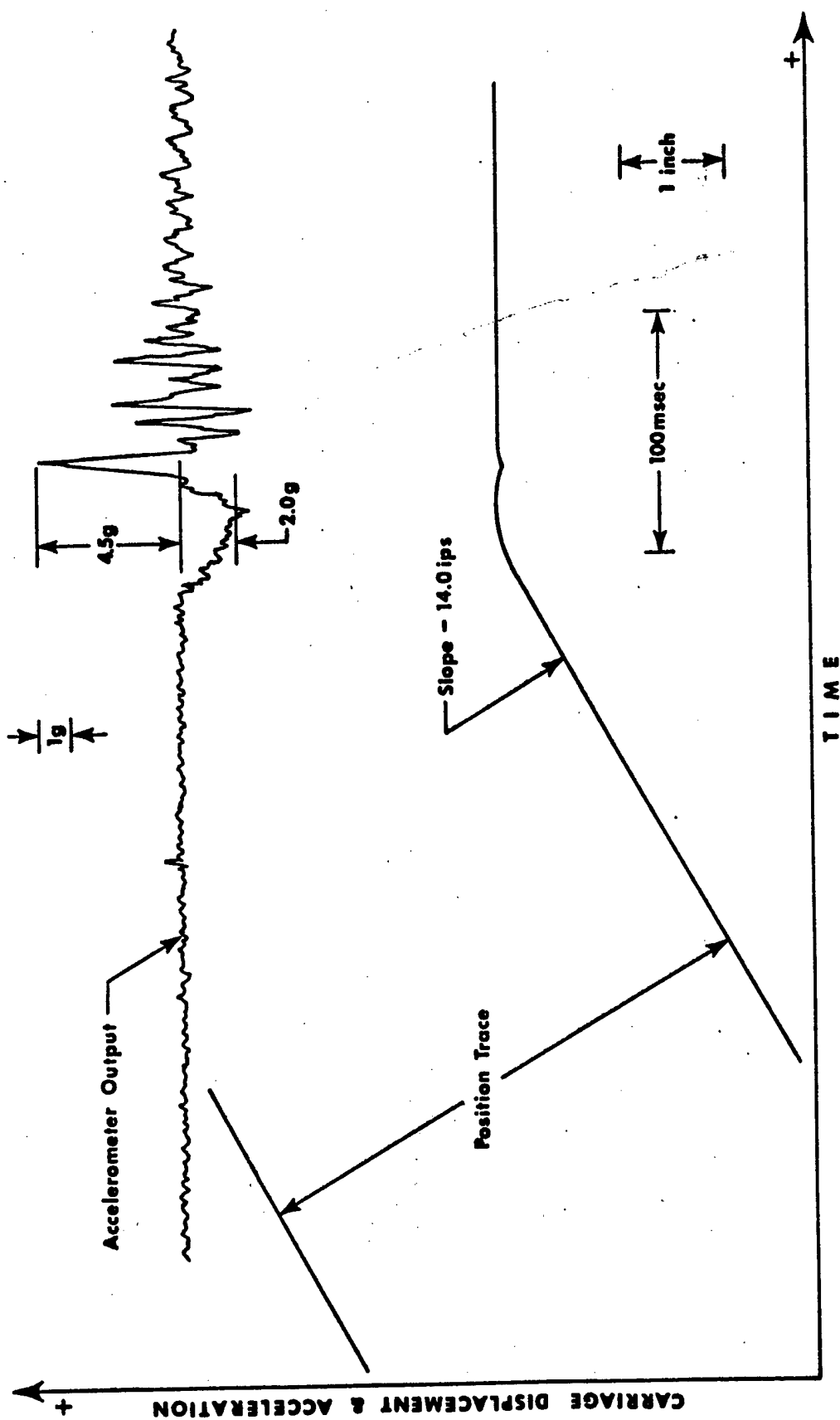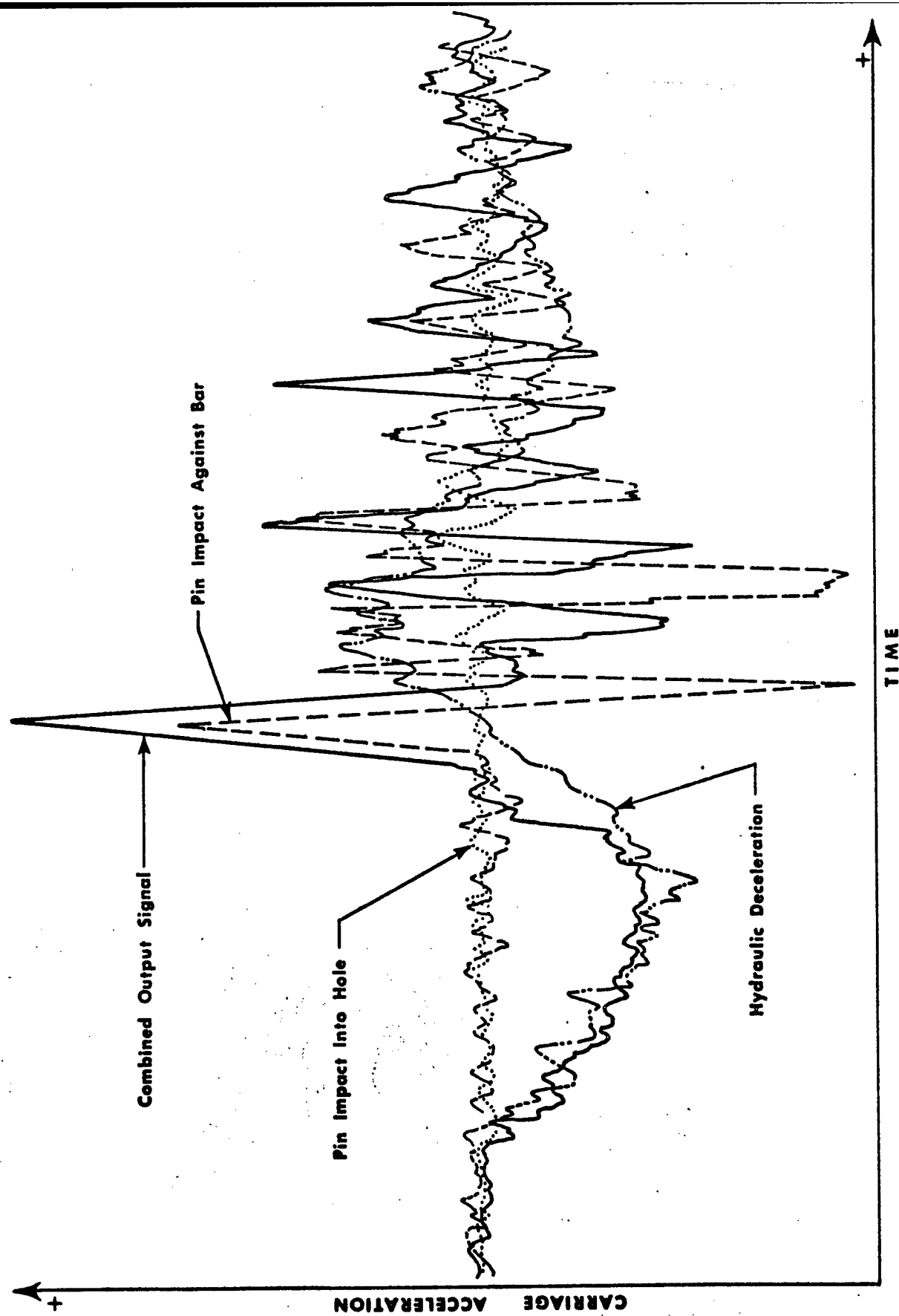
16

FIGURE 5. RESULTANT INTERIM DECELERATION

17

FIGURE 6. INTERIM DECELERATION COMPOSITE

18

On the other hand, the hydraulic deceleration of the carriage is a direct function of its speed as indicated by the data in Table 2.

Another factor which influences the shape of the resultant accelerometer output signal is the interaction of the various frequencies. If summing signals undergo constructive interference the resulting amplitude of the signal is substantially greater than if the signals undergo destructive interference. Hence, the resultant output signal varies over a quite large range of amplitudes during different pinning processes.

III.A.3. Interim Acceleration

The acceleration of the carriage from an interim strut position was very similar to the initial acceleration. The accelerometer detected a noise signal caused by the hydraulic valving and a signal caused by the mechanical acceleration of the carriage. An additional acceleration was produced when the locking pin was retracted. These effects are again discussed separately in the following paragraphs.

Figure 7 is a replica of the accelerometer output signal produced when the carriage was accelerated from rest at strut 3 to 20.4 ips without the use of the locking pin. The noise signal caused by the hydraulic valving occurred about 60 msec before the carriage began to move. Its magnitude was approximately the same as that superimposed on the initial acceleration signal although its frequencies had shifted. The fundamental frequency of the noise signal in Figure 7 was about 100 hz and its first overtone was 200 hz. These frequencies were considerably higher than those of the initial acceleration noise signal (72 and 144 hz).
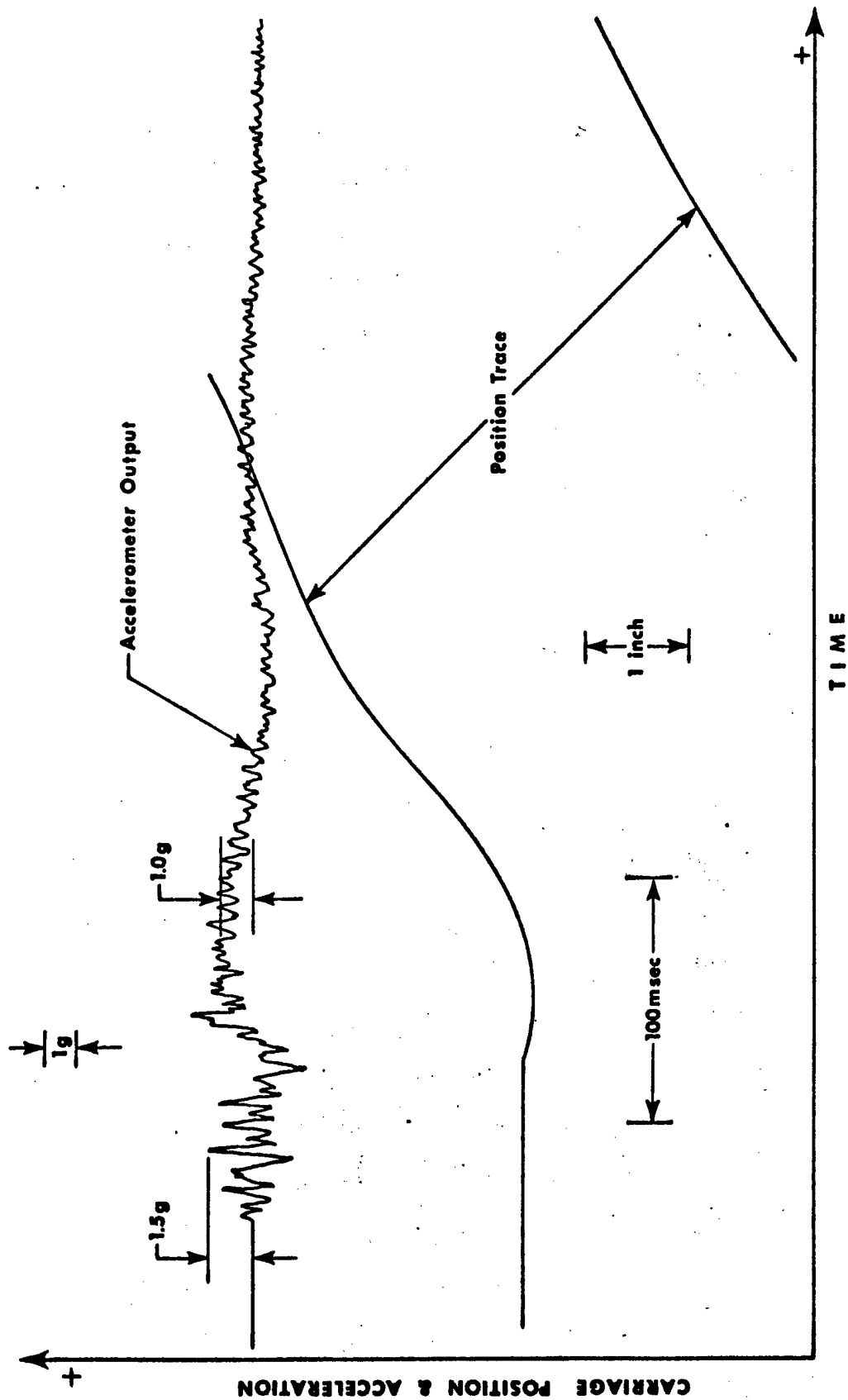
FIGURE 7. INTERIM TRANSVERSE ACCELERATION WITHOUT PIN USAGE

20

This presumably was caused by the different path length which the noise had to travel to the accelerometer which was still mounted on strut 5 and was moving away from the hydraulic valves. The overall shape of the two noise signals was almost identical.

The mechanical acceleration of the carriage to 20.4 ips created a maximum g-load of about 1 g and it occurred about 50 msec after the carriage began to move. As with the initial acceleration, steady carriage speed was attained after several cycles of velocity overshoot.

The next component of acceleration to be examined is that produced when the locking pin is retracted. Figure 8 shows a typical accelerometer response when the carriage was hydraulically locked in position and the alignment pin retracted. Since the pin was seated in the alignment hole in a slightly cocked position (as described in the previous section) the initial movement of the pin produced a significant noise signal with a magnitude of about 1.5 g and a frequency of about 330 hz.

The acceleration signal in Figure 9 shows the pin-produced noise (330 hz) superimposed on the hydraulic valving noise (100 hz) just prior to carriage acceleration. The two components were readily separable during a given carriage traverse since as the pinning maneuver proceeded from one strut to the next the frequency of the hydraulic valving noise increased. On the other hand as the traverse proceeded, the accelerometer which was mounted on strut 5 approached the pin and the magnitude of the pin retraction noise signal increased significantly. Its magnitude was
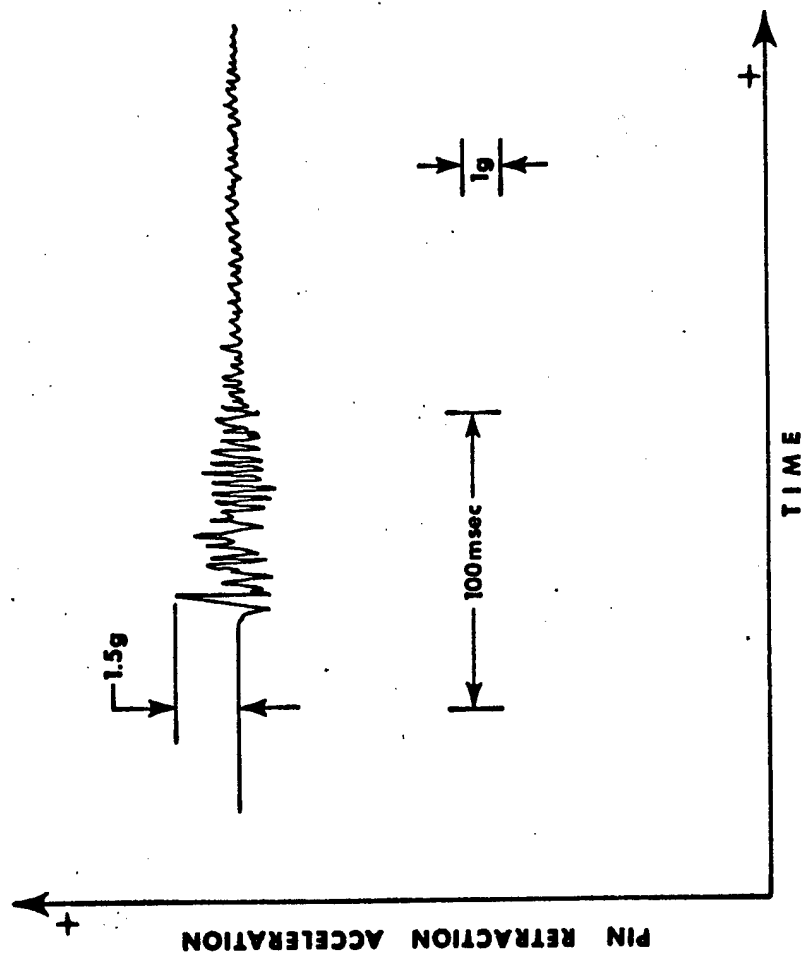
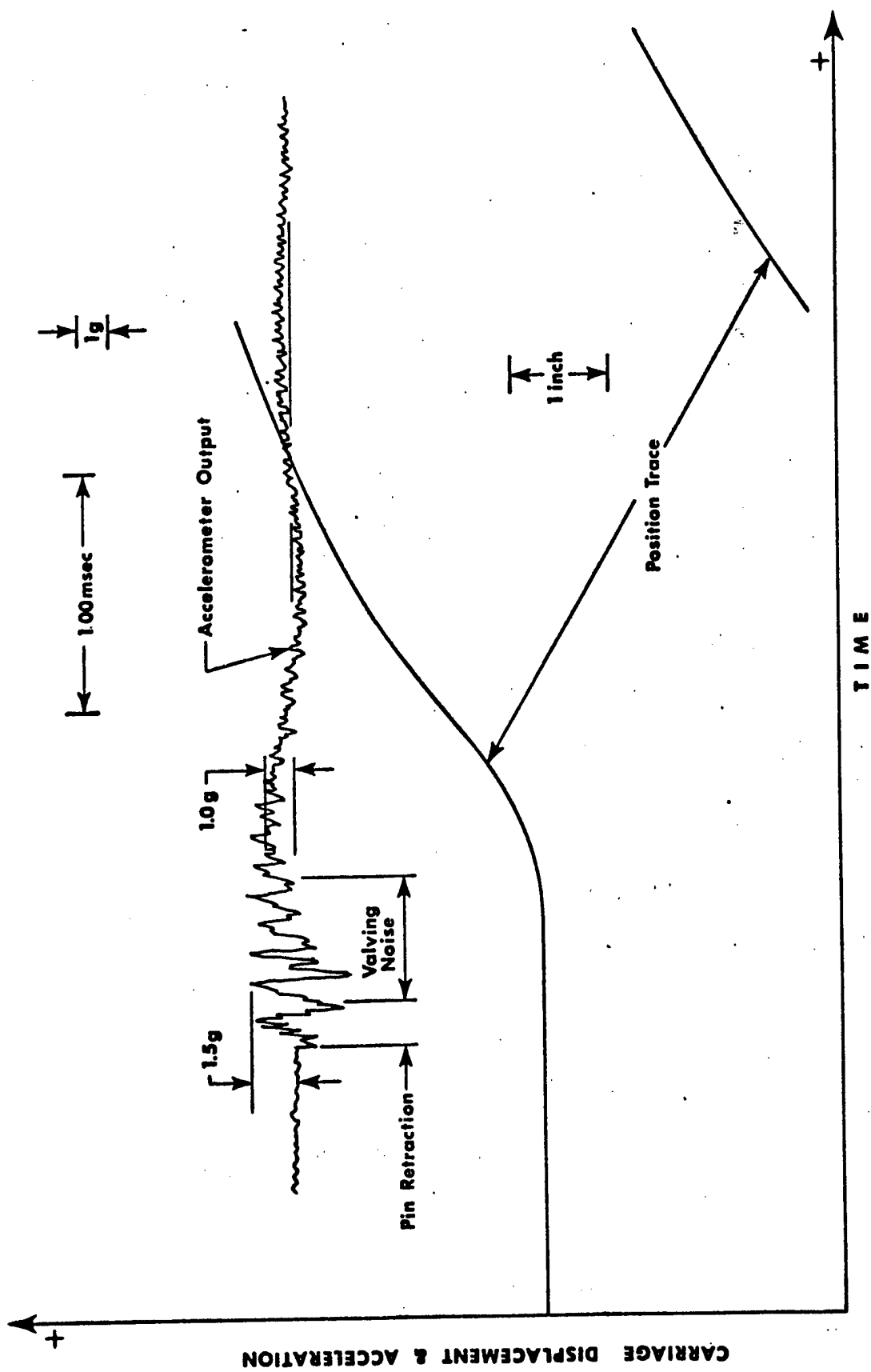FIGURE 8. PIN RETRACTION ACCELERATION, CARRIAGE HYDRAULICALLY LOCKED

22

FIGURE 9. PIN RETRACTION AND CARRIAGE ACCELERATION

23

about 0.8 g at strut 1 and about 2.9 g at strut 5.

All of this extraneous noise was attenuated during the first 75 msec of the acceleration sequence. Hence, the actual mechanical acceleration of the carriage is shown clearly on the accelerometer output. The range of accelerations produced by the interim acceleration of the carriage to various speeds was identical to those g-loadings produced during initial acceleration.

III.A.4. Final Deceleration

Figure 10 is a selected accelerometer trace which shows the final carriage deceleration process from about 60 ips. The process begins as a steel plate on the leading edge of the carriage contacts the fully extended shock absorber. The noise of impact can be seen on the trace. Following the initial impact the absorber begins to compress and the carriage begins to decelerate, very slowly at first, and then quite rapidly. About 75 msec after initial impact with the shock absorber a peak deceleration of about 6 g occurred. The carriage continues to decelerate until it comes to rest when the shock absorber bottoms. The trace in Figure 10 shows that a deceleration of almost 8 g occurred when the absorber bottomed. The frequencies of the noise and mechanical deceleration signals were random. The portion of the accelerometer trace following the time when the carriage was completely stopped was simply vibration reflections within the carriage structure.

The particular model of shock absorber used on the RENT carriage permits adjustment for operation over a fairly broad range of carriage velocities. The data presented in Figure 10 indicates that the absorber could have been adjusted to be a bit more firm. Very little
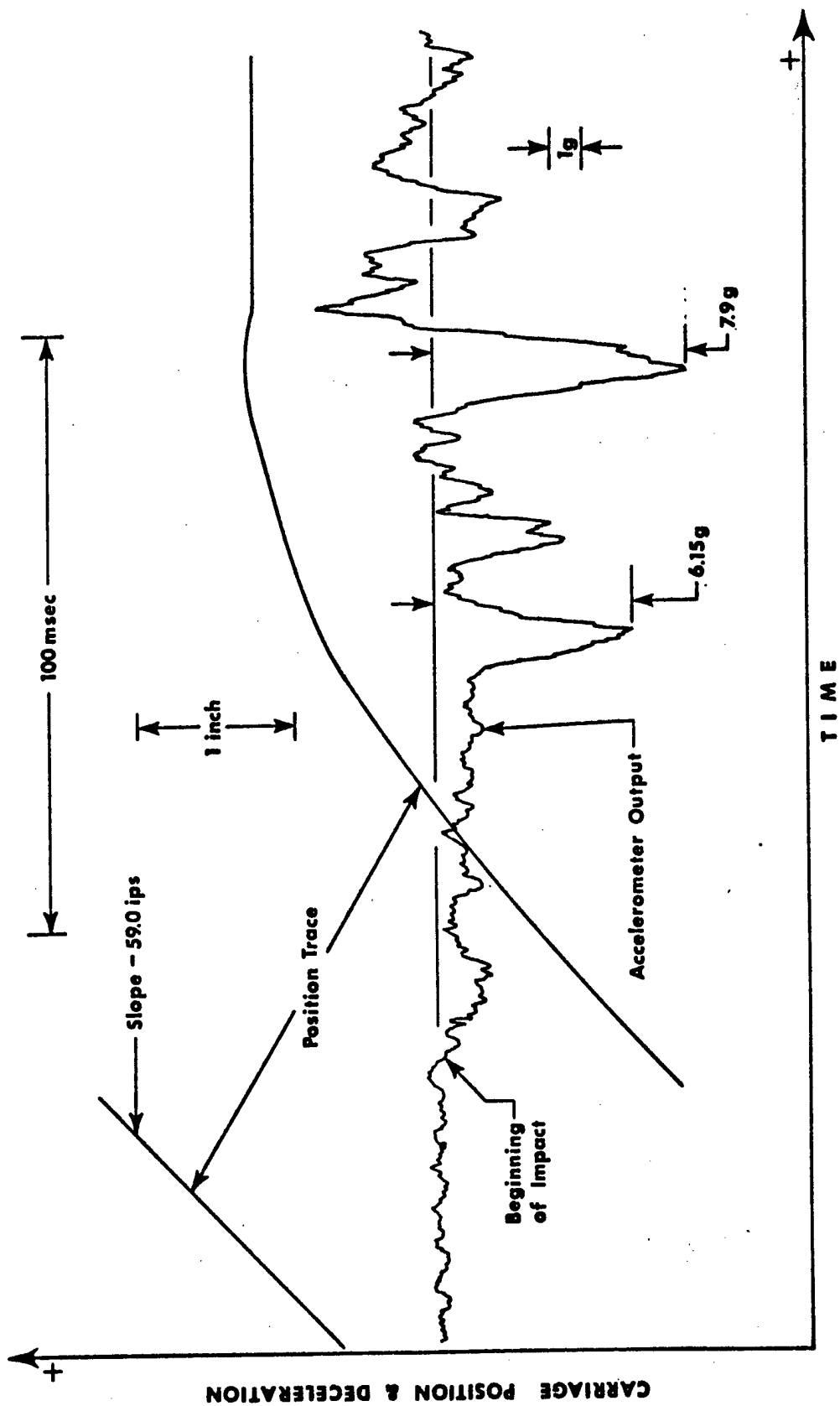
24

FIGURE 10. FINAL TRANSVERSE DECELERATION.

25

deceleration occurred during the first 75 msec. The carriage then slowed quickly producing a deceleration of about 6 g. By adjusting the absorber, carriage velocity could be reduced even further prior to bottoming of the absorber. It would probably be best to decrease the bottoming deceleration to no more than about 4 g.

The data presented in Table 3 shows the deceleration occurring at absorber bottoming over a range of carriage velocities at the same absorber adjustment as used above. At the low end of the velocity range almost no carriage deceleration occurred prior to bottoming of the piston. This is not unexpected since the adjustment had been made for high speed operation. Above 30 ips the data in Table 3 provides evidence of the proper functioning of the absorber. With the present adjustment the bottoming g-loading is limited to about 8 1/2 g at a carriage speed of about 35 ips. As carriage speed further increases the bottoming deceleration holds essentially constant as more and more of the carriage kinetic energy is absorbed prior to bottoming.

III.B. General Description of The Acceleration/Deceleration Pattern During a Two-Position Axial Strut Movement

Once the carriage has been pinned on a particular strut center-line, the axial drive interlock system permits that strut to be axially driven. The axial drive capability is used in one of two ways. It can be used to continuously track, thereby keeping the ablating nose of a model within the flow field test rhombus. This is done by using two light sensor signals in a feedback circuit which in turn governs the hydraulic servo system. This mode of axial drive does not produce significant accelerations and hence will not be considered in this report.

26

TABLE 3   SHOCK ABSORBER DECELERATIONS.*

Carriage Velocity	Bottoming Deceleration
(ips)	(g)
7.55	2.80
14.5	4.80
16.1	5.35
19.7	5.65
22.6	6.40
25.0	6.85
30.2	7.90
35.3	8.40
36.0	8.60
43.5	8.00
59.0	7.95

* More recent data indicated that at the time this data was acquired
  the shock absorber was beginning to malfunction. Replacement
  and subsequent checkout revealed that the absorber normally func-
  tions over a broader velocity range and somewhat reduces all decel-
  erations in the final deceleration process.

The second operational mode of the axial drive system is two-position. The strut drives forward from a rear to a front position. Maximum acceleration occurs about 6 msec after the strut begins to move. Deceleration at or near the forward position is initiated either mechanically or hydraulically. Mechanical deceleration occurs effectively instantaneously when the strut base encounters a mechanical stop. The resulting decelerations can be quite severe depending on the strut speed.

In a situation where lower strut decelerations are required, activation of a hydraulic servo system permits the rather gradual deceleration of the strut to rest. This, of course, considerably increases the time required to complete the axial strut movement.

When both a time and g-load limit must be considered, mechanical and hydraulic decelerations can be combined to achieve an optimum result.

III.B.1. Acceleration From Rear Axial Position

The acceleration and axial position traces shown in Figure 11 are typical of those produced when any given strut is axially driven from a rear stationary position. The accelerometer was mounted with its axis of maximum sensitivity parallel to the axial centerline of the strut.

Within five or six msec after the strut began to move, a peak acceleration of 9.6 g was recorded as the strut accelerated to a velocity of 17.2 ips.

As is evident from the data shown in Table 4, the acceleration is a direct function of the strut velocity since the acceleration distance is always extremely short.
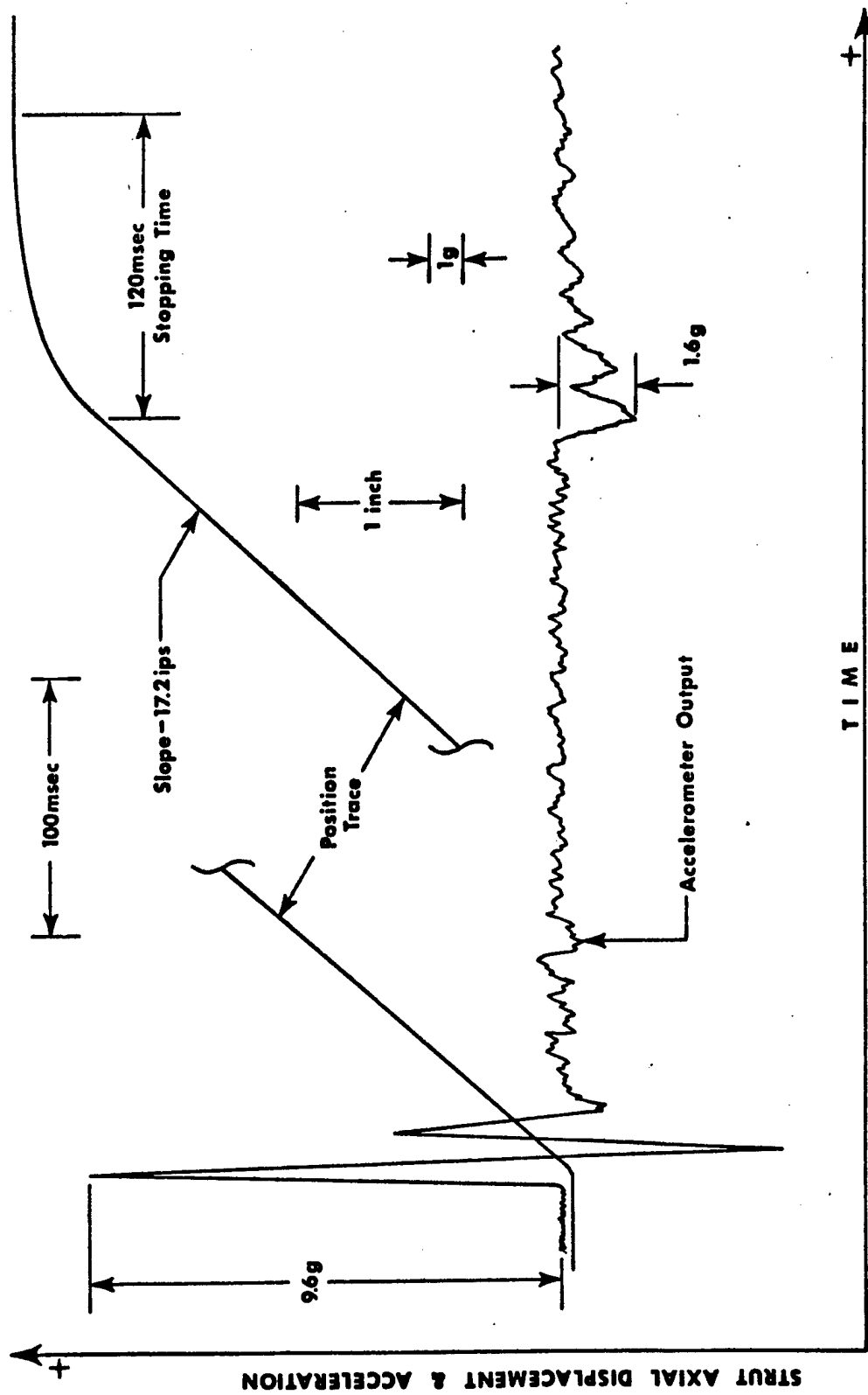
FIGURE 11. INITIAL AXIAL ACCELERATION AND HYDRAULIC DECELERATION

29

TABLE 4 AXIAL DRIVE ACCELERATIONS

Strut Velocity (ips)	Initial Acceleration (g)	Hydraulic Deceleration a (g)	Mechanical Deceleration b (g)
4.01	2.30	0	3.67
5.40	3.25	0	5.40
6.80	3.90	-	7.50
8.15	4.60	-	9.30
10.0	6.00	0	11.8
12.4	7.30	-	12.5
17.2 (Figure 11)	9.57	1.60	-
17.2	9.60	1.67[c]	1.00[c]
24.6	10.3	2.67[d]	10.8[d]

a Programmed for servo control stop 1/2" short of front limit.

b No servo control. Full stop occurred when front limit was hit.

c Programmed for servo control about 1/2" short of front limit. Gain adjusted to allow limit hit.

d Programmed for servo control about 1" after leaving rear position. Gain adjusted to allow limit hi

Even after acceleration to constant velocity has been completed, the accelerometer output signal in Figure 11 shows a significant noise component throughout the axial traverse. This noise most likely results from the instrument's extension cable dragging across the model support carriage. This noise stops just as the strut begins its rapid deceleration at the forward position and therefore does not obscure the deceleration signal from the accelerometer.

III.B.2. Deceleration at Front Axial Position

The axial position and accelerometer traces on Figure 11 show the results of a hydraulic deceleration at the forward axial position. As the strut approached the prescribed set point the Moog servo valve began to slow the strut. This servo process required about 120 msec to bring the strut to a complete stop. The cyclic pattern of the accelerometer signal was caused by vibration reflections (50 hz) super-imposed on the exponential deceleration curve.

Hydraulic deceleration of the strut from a speed of 17.2 ips resulted in a g-loading of 1.6 g. As the results shown in Table 4 indicate, the strut deceleration (both hydraulic and mechanical) was a function of strut velocity just as for the acceleration from the rear strut position. Also, the three non-zero values of hydraulic deceleration shown in Table 4 represent three different servo system settings. Servo deceleration from 17.2 ips to rest was programmed to occur over only the last half inch of strut travel. The servo system set-up for the final entry in Table 4 was to slow the carriage from about 25 ips to just under 10 ips over a length of almost 4.5 inches. The strut base was then permitted to impact the forward limit plate, creating a deceleration of over 10 g. In actual

practice there is an infinite number of ways to employ the servo system to decelerate the forward-moving strut.

Figure 12 shows the results of allowing a full six inches of travel (stop-to-stop) on the axial traverse without using the servo system. The acceleration from the rear position was similar to that described above. The noise produced by the dragging cable was also evident. As the strut base encountered the forward limit, the position trace indicated a very sudden stop over a very short distance. The associated g-loading was 3.67 g even at this low strut velocity of 4.01 ips.

Figure 13 shows the combination result where the strut was partially decelerated hydraulically from 17.2 ips before it encountered the mechanical stop. This effectively reduced the total stopping time from 120 msec for a purely hydraulic stop at 17.2 ips to 85 msec for the combination stop from the same velocity. The maximum g-loading was 1.6 g for the former and only increased to 1.67 g for the latter deceleration.
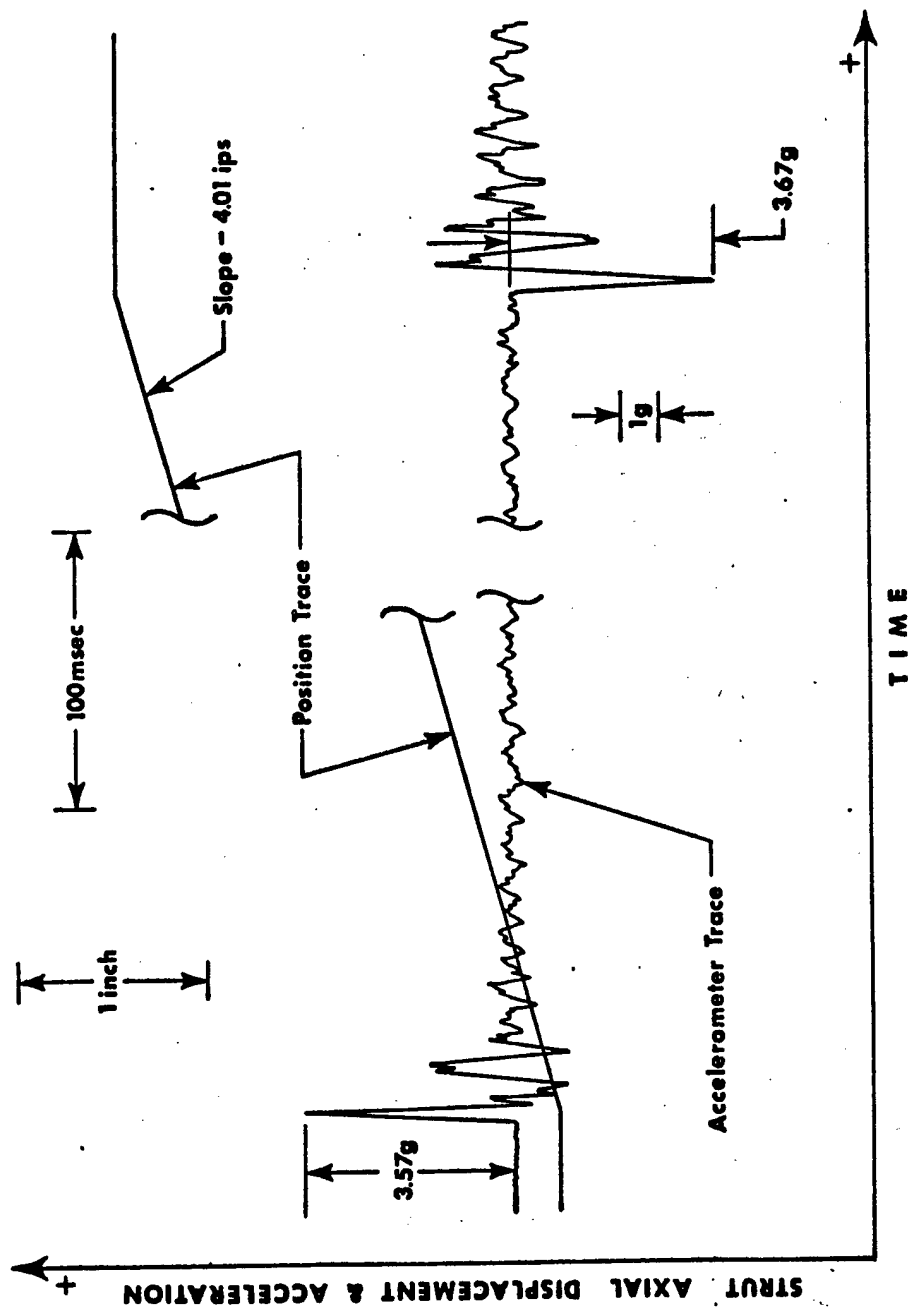
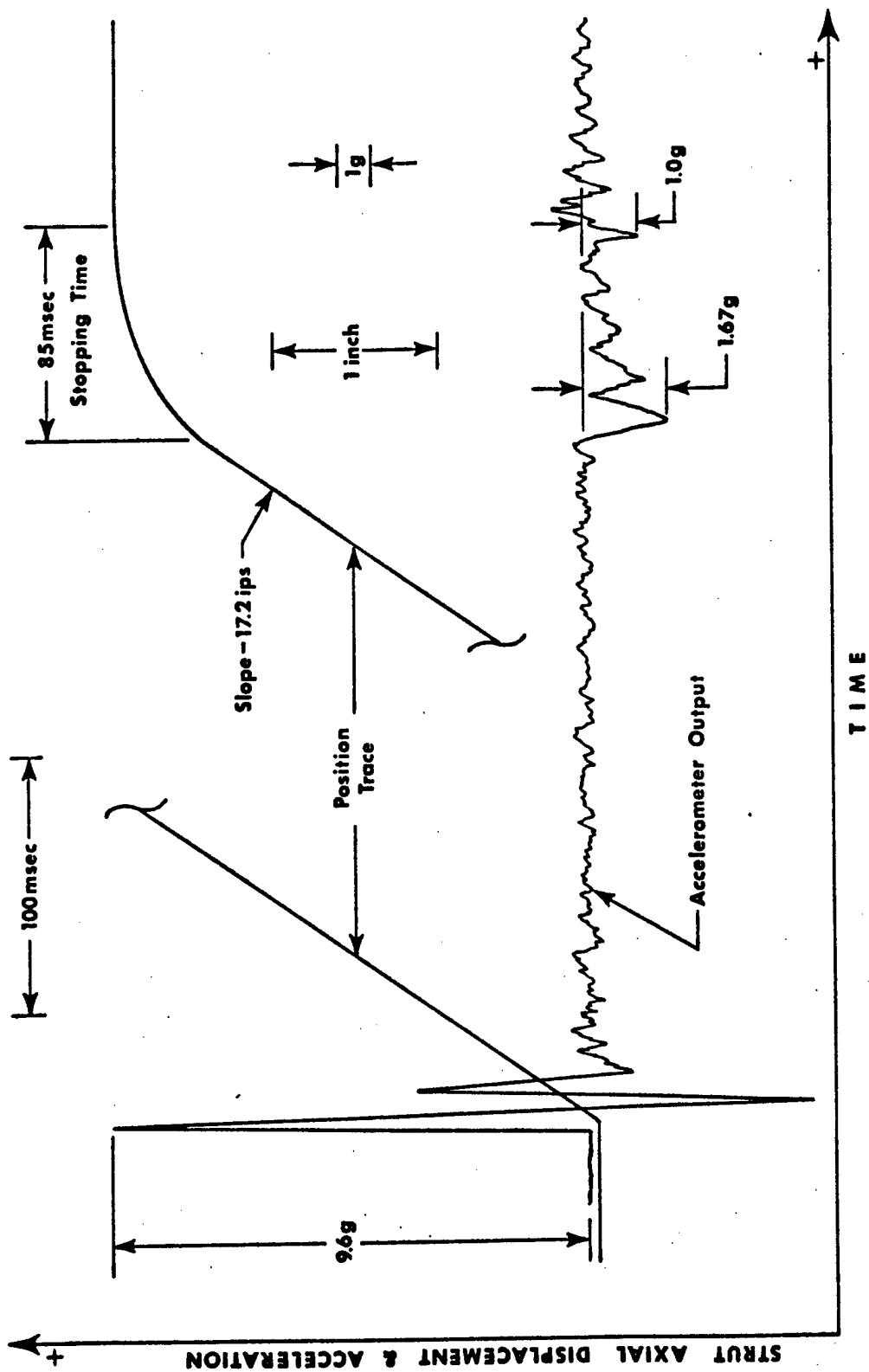FIGURE 12. AXIAL DECELERATION AT MECHANICAL LIMIT

33

FIGURE 13. HYDRAULIC AND MECHANICAL AXIAL DECELERATION

IV. SUMMARY AND CONCLUSIONS

A large block of acceleration data has been assembled and analyzed. This data spans the normal operating range of transverse carriage and axial strut movement.

Accelerations were recorded during five particular maneuvers in a lateral carriage traverse. The first of these were those produced during the initial carriage start. The data presented indicates that the accelerations were quite modest over the entire speed range of the carriage which was investigated. An acceleration to 3.12 ips created a g-load of 0.20 g and to 65.4 ips only 2.00 g. Thus, g-loads produced on test models during initial carriage acceleration present no particular problems.

The accelerations produced during the interim acceleration likewise were only modest and of no real concern.

A third carriage maneuver which was investigated was the final deceleration to rest against the shock absorber seat. The g-loads produced were more severe, ranging from 2.8 g at 7.55 ips to 7.95 g at 59.0 ips. It should be stressed, however, that the data in Table 3 for speeds below 40 ips were a result of operating the shock absorber "off-design". Proper adjustment of the internal orifices can substantially reduce the magnitude of the final deceleration by making the absorber effective over its entire four inch travel length. This adjustment is easily done by turning a single external screw. It became apparent during this study that the present manner of setting the absorber for a given carriage speed is totally inadequate. Adjustment based on the shape of the position trace cannot suffice since this parameter is far too insensitive. It is

strongly recommended that future adjustments be made using the accelero-
meter output to minimize g-loads during the final deceleration process.

The last transverse maneuver examined in detail, the interim decelera-
tion at a particular strut, has the potential of generating the most
severe g-loads in normal transverse carriage movement. The interim
deceleration consists of hydraulic isolation and mechanical pinning.
The process of hydraulically isolating the carriage produced maximum
decelerations ranging from 0.60 g at 2.94 ips to 5.65 g at 38.4 ips. The
recorded values were quite repeatable.

On the other hand, pinning of the carriage on a particular strut
centerline posed the problem of unrepeatable vertical g-loads up to 12 g.
When the alignment pin and hole were badly misaligned, which could be
expected to happen at high carriage speed, near-maximum g-loading occurred.
At lower speeds and better alignment lesser g-loads occurred.

The net result of the interim deceleration investigation is that while
it is recognized as the most probable source of design-limit g-loads for
model and/or instrumentation design, the predictability of the absolute
value of these limits for a particular traverse are quite poorly defined.
Adequate operational procedure precautions generally will allow holding
these g-loads under 5 g maximum. In the situation where the model being
tested is at all fragile it is necessary to exercise extreme care in
aligning the pin hole and pin prior to its insertion.

The two-position mode of model strut axial drive can produce signifi-
cant axial g-loads. The acceleration from a rear position occurs very
quickly and thus the g-loads are correspondingly quite large. Axial loads

ranged from 2.3 g at 4.01 ips to 10.3 g at 24.6 ips.

The mechanical deceleration at the forward position, while minimizing the time of travel, maximizes the deceleration loads. Loads ranged from 3.67 g at 4.01 ips to 12.5 g at 12.4 ips. Mechanical stops from higher speeds were not and should not be attempted so that damage to the axial drive system can be avoided.

Using a hydraulic servo deceleration at the forward position has the advantage of significantly reducing the deceleration g-loads. However, the time to stop increases as a direct function of the amount of servo control.

Results also were presented for a combination stop wherein the strut velocity was reduced substantially by the servo system prior to striking the mechanical stop. The result was about a one-third savings in stopping time over the full servo stop with only about a five per cent increase in g-load. This is the recommended mode of two-position axial drive whenever stopping time is not critical.